

VALIDATING FLUENT FOR THE FLOW OF GRANULAR MATERIALS IN AERIAL SPREADERS

R. K. Bansal, J. T. Walker, D. R. Gardisser, T. E. Grift

ABSTRACT. A simulation model for predicting the velocity vectors of fertilizer particles emanating from an aerial spreader was developed using a commercial software package FLUENT version 4.32. Simulation results for urea particles emanating from a curved duct were compared with laboratory results. The particle size (geometric mean particle diameters) ranged from 1.30 mm to 2.82 mm and the air velocity at the inlet of a curved duct was varied from 42 m/s to 62 m/s. FLUENT always predicted lower particle velocities than were measured in the laboratory. The difference was attributed to uneven shape of the particles and modeling errors. FLUENT predicted particle velocities could be corrected with a correction factor specific to a fertilizer. For materials having particles of different shapes the value for correction factor would be different. The particle velocity was found to be linearly related to the air velocity. The effect of the particle size on its velocity was quadratic, with smaller particles attaining higher velocities at the exit from the duct than did the larger particles. **Keywords.** Fertilizer, Aerial, Spreader, FLUENT.

Aerial application of fertilizer and granular pesticides to forests and crops, such as rice, cotton, wheat, and soybeans, has been practiced in the United States and other countries for decades. Aerial application is fast, economical and permits applications to areas that may not be easily accessible by any other means. Whereas aerial application has these and many other advantages, the agricultural aviation industry today is under constant pressure to be more efficient. There is considerable internal competition within the industry requiring that pilots do a professional job to stay competitive. This includes applying liquid and granular materials more uniformly on the target area and reducing waste. There are also growing environmental concerns about potential pollution of air and groundwater from either excessive or non-target applications. These concerns have necessitated improvements in the technology and the knowledge about the physical processes involved in the distribution of applied materials.

Research on improving the distribution patterns of agricultural aircraft dispersal systems started in the early 1950s (Texas A&M University, 1956; Henry, 1962; Bilanski et al., 1962; Akesson and Yates, 1964). Early efforts were mostly directed toward quantification of variations in the distribution pattern and developing knowledge about the factors responsible for them. Henry

(1962), Akesson and Yates (1964), and Brazelton et al. (1968) compared spreader designs based on data collected in field studies. They used empirical methods to characterize the effect of spreader design features as well as operating conditions on the distribution pattern of granular fertilizer. During the 1970-1990 period, there was greater emphasis on applying the principles of mechanics and aerodynamics to characterize the dispersion of granular material from tractor-mounted and aerial spreaders. West (1972) and Law and Collier (1973) studied the aerodynamic drag force on agricultural materials as a function of particle diameter, density, and shape. They attempted to develop accurate models for predicting the trajectory of fertilizer particles released at a particular velocity and height above the ground. Similarly, Mennel and Reece (1963) and Griffis et al. (1983) modeled the trajectory of fertilizer particles released from rotary spreaders operating near the ground. However, all of these studies were based on a single particle approach, and the effect of turbulence was not considered.

Walker and Gardisser (1989) applied the idea of particle trajectory calculations to particle deposition pattern analysis. They adapted a computer program AGDISP (Bilanin et al., 1989) to calculate the expected overall distribution pattern for different swath widths, based on the observed material deposition pattern from one pass of the aircraft. The effect of operating conditions, such as wind velocity and direction and adjustment of vanes at the front end of the spreader, could be seen on the distribution pattern. This approach helped improve adjustments on the spreaders (Gardisser and Walker, 1990). The effect of the physical characteristics of the applied material, spreader design features, and operating conditions on the distribution pattern is not yet well understood. One of the most serious limitations is the lack of information about the velocity and the angle of ejection of particles from the spreader. These two factors largely determine their trajectories in the air and their deposition pattern on the ground.

Article was submitted for publication in May 1997; reviewed and approved for publication by the Power & Machinery Div. of ASAE in December 1997.

Names of commercial products are used in this article for descriptive purpose only, and do not imply endorsement over similar products.

The authors are **Ram K. Bansal**, ASAE Member, Research Associate, **Joel T. Walker**, ASAE Member Engineer, Professor, **Dennis R. Gardisser**, ASAE Member Engineer, Extension Agricultural Engineer, and **Ton E. Grift**, Graduate Assistant, Biological and Agricultural Engineering Department, University of Arkansas, Fayetteville, Ark. **Corresponding author:** Dr. Joel T. Walker, Biological and Agricultural Engineering Dept., 203 Engineering Hall, University of Arkansas, Fayetteville, AR 72701; tel: (501) 575-7400; fax: (501) 575-2846; e-mail: jtw@engr.uark.edu.

The velocity vectors of particles emanating from an aerial spreader depend upon a number of factors such as density, size and shape of individual particles, air velocity distribution inside the spreader ducts and the vane curvature. They also depend upon the mass flow rate of the applied material and the starting location of individual particles where they were introduced in the air stream. Hence, the acceleration of particles in the spreader is a function of several variables and an analytical solution to this problem may not be possible. In contrast, a computer simulation can be remarkably simple for predicting particle velocity vectors at any point inside the spreader and at the exit plane. However, a simulation model must be validated before applying it to a real situation.

The overall objective of the research reported in this article was to develop a simulation model for the flow of granular materials in aerial spreaders, so that the velocity vectors and the location of particles emanating from the spreader could be accurately predicted. For this purpose, a commercial computational fluid dynamics software package, FLUENT version 4.32 (Fluent Inc., Lebanon, NH), was used. Tests were conducted in the laboratory to measure velocity of urea particles emanating from a curved duct that resembles one of the ducts of a typical aerial spreader. Particle velocities predicted by the model were compared with laboratory results. The effects of the particle size and the air velocity at the duct inlet on the velocity of particles emanating from the curved duct were also studied.

THE SIMULATION PROCEDURE

The FLUENT procedure for simulating the transport of two or more fluids together is called dispersed phase simulation. One of those fluids is the primary phase because it is the prime mover causing the flow to occur. The other fluid, referred to as the dispersed phase, can be either liquid (droplets), gas, or discrete solid particles. The problem is set in the Lagrangian frame that treats the primary fluid as a continuum and predicts the trajectory of a particle in the computational domain as a result of forces acting on it (Durst et al., 1984). A solid-fluid flow is simulated by assuming different starting positions of several particles and their initial boundary conditions. Each particle represents a continuous flow of similar particles starting from the same location at a specified mass flow rate. The general procedure for solving the problem in FLUENT is to establish the flow fields for the primary fluid in the computational domain first and then introduce the dispersed phase. The initial location of particles can be anywhere inside the computational domain specified by Cartesian coordinates for injection points. Input values are required for particle density, mass flow rate, and initial velocity vectors in the x, y, and z directions. Any of the variables can be assigned a range of values. FLUENT uses a linear scaling for assigning values for that particular variable to each injection point. The force exerted by the fluid on the dispersed phase is calculated from the following equation (Fluent Inc., 1995, pp. 19-116).

$$F = \sum \frac{3\mu C_d R_e}{4\rho_q d_q^2} (u_f - u_q) m_q \Delta t \quad (1)$$

where

μ = viscosity of the fluid

C_d = coefficient of drag

R_e = Reynolds number

u_f = instantaneous velocity of the fluid in x coordinate

u_q = instantaneous velocity of the particle in x coordinate

Δt = time step

ρ_q , d_q , and m_q are the particle density, diameter, and mass flow rate, respectively.

The size of the particle and the difference between the fluid and the particle velocities ($u_q - u_f$) play a major role in the transfer of momentum from fluid to particles.

Some of the major advantages of using a commercial computer program such as FLUENT are: (1) the benefit of features already tested and incorporated in the program; (2) the possibility of simulating the flow of a large number of particles together rather than taking a single particle approach; and (3) saving results such as velocity vectors and the relative pressure for the fluid and velocity vectors, mass concentration and trajectory of particles at any location inside the geometry in both graphical and numerical forms. The steps required for simulating a dispersed phase flow in FLUENT are: (1) creating a geometric representation of the physical domain; (2) selecting a suitable solution model depending upon the nature of the flow; (3) setting appropriate boundary conditions and the physical constants for the flow conditions and fluid properties; (4) solving for the flow fields of the primary fluid; (5) defining the particles starting locations, velocities, size, mass flow rate and physical properties; and (6) solving for the particle trajectories.

Figure 1 shows the outline of an eleven-duct aerial spreader (model 23501, Transland Inc., Harbor City, Calif.). This spreader is about 1 m wide and 360 mm high at the front end and 3.9 m wide and 116 mm high at the rear end. The length of the spreader is about 1 m. Aerial spreaders are made from stainless steel sheet to provide durability and avoid corrosion. The inside space is divided into as many as 13 ducts that curve out to the left or the right in order to guide the flow of material to both sides of the aircraft. However, eleven-duct spreaders are more common in Arkansas for application of fertilizers. Out of eleven ducts, four ducts on one side of the spreader are the mirror images of four ducts on the other side. The remaining three ducts in the middle section are asymmetrical. They are made to direct more material to the right side of the aircraft to compensate for the effect of the propeller wake. An additional feature of the spreader ducts is that for some distance into the duct from the front end,

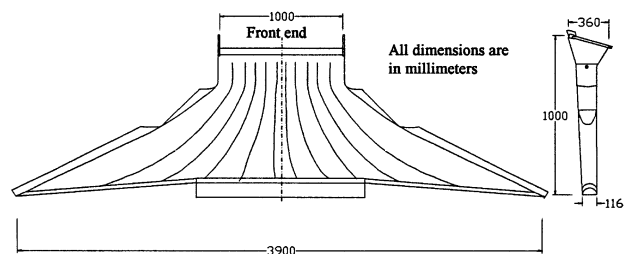


Figure 1—A plan view of an eleven-duct aerial spreader.

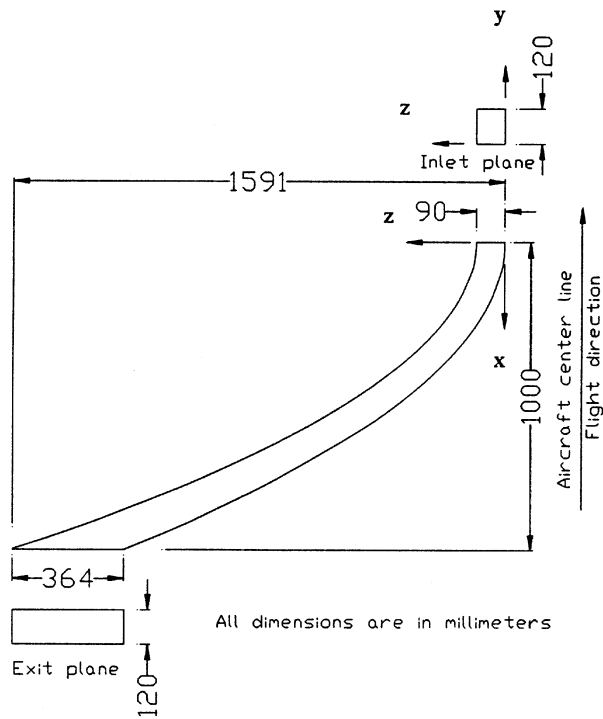


Figure 2—Overall dimensions of a curved duct modeled in FLUENT.

the cross-sectional area of the duct increases very slowly as the distance between the side walls remains nearly constant. This part of the spreader is referred to as the throat. Further along the length, the side walls diverge rapidly causing a rapid area expansion of the duct. The shape of a curved duct modeled in FLUENT is shown figure 2. The side walls of this duct had parabolic curvatures that resemble the first and the second ducts from the left side on the aerial spreader (fig. 1). The curved duct had a constant height of 120 mm. It has a 90 mm wide inlet and a 364 mm wide outlet measured parallel to the inlet face (not the cross-section). The coordinate system used in FLUENT is also shown in figure 2. The origin coincides with the point where the lower edge of the outer side wall begins. The z and the y coordinates run along the width and the height of the inlet plane. The x coordinate is perpendicular to the inlet plane. The velocity vectors are designated as u, v, and w in x, y, and z directions, respectively.

This problem was set up in FLUENT as a turbulent flow isentropic model. For the turbulence coefficient that determines air velocity fluctuations from its mean velocity, the default value of 10% was used. Air velocity at the inlet of the curved duct was varied in four steps: 42, 46, 56, and 62 m/s corresponding to agricultural aircraft airspeed in the range of 150 to 220 km/h. Typically agricultural aircraft are operated at an airspeed of 190 to 210 km/h. At these velocities, the airflow inside the duct was expected to be turbulent. However, the Mach number at the highest air velocity of 62 m/s was calculated as 0.18, which is sufficiently low for the flow to remain incompressible. A separate FLUENT solution was obtained for each of the four inlet air velocities.

Table 1. Particle size distribution in a urea sample

Sieve No.	Opening Size		GMD*	Retained on the Screen (g)	Mass as % of Total	Cumulative Percentage
	(in.)	(mm)				
6	0.1320	3.35	3.66	20	1.76	1.76
8	0.0937	2.38	2.82	422	37.08	38.84
10	0.0799	2.03	2.20	432	37.96	76.80
12	0.0661	1.68	1.85	222	19.51	96.31
14	0.0555	1.41	1.54	36	3.16	99.47
16	0.0469	1.19	1.30	4	0.35	99.82
Pan	None					100.00

* Geometric mean diameter of urea particles.

A urea sample collected from aerial applicators in Arkansas was screened through a set of U.S. standard sieves no. 6 through 16 to determine the mass fraction in different particle size groups (table 1). Geometric mean diameter (GMD) for urea particles retained on sieves was calculated using the following equation (ASAE Standard S319.1):

$$d = (d_i \times d_{i+1})^{0.5} \quad (2)$$

where d is the geometric mean diameter, d_i is the opening size of the sieve and d_{i+1} is the size of openings in the next larger sieve. GMD was then used for specifying the urea particle size both in FLUENT and in the laboratory tests. Fifteen urea particles (referred to as injections in FLUENT) were introduced for each size group represented by its GMD across the width of the duct at the air inlet end. The size groups specified were 1.30, 1.54, 1.85, 2.20, and 2.82 mm. The largest size group of 3.66 mm was not used because there were no comparable data for this size from laboratory tests as explained later in this article. The reason for 15 particles in each group was to have an adequate reflection of air velocity variations inside the curved duct on particle velocities at the exit plane. The total mass flow rate in all particle sizes was assumed to be 1 kg/s which roughly corresponded to a urea application rate of 110 kg/ha from an agricultural aircraft. The coefficient of restitution for urea particles on stainless steel was assumed as 0.30 based on the findings of Hofstee (1992). Similarly, urea particle density was assumed to be 1220 kg/m³ as reported by Hoffmeister (1979).

The FLUENT solution for particle trajectories contained time, location, and velocity data in Cartesian coordinates for each injection from the beginning until the particle left the computational domain. This information was used in FLUENT for generating particle tracks and concentration contours. It could also be extracted as a text file for individual injections. This facility in FLUENT permitted saving particle velocity vectors in Cartesian coordinates along the trajectories in the curved duct. Thus for 15 particle injections in each of five size groups, velocity vectors for a total of 75 urea particles were saved at the exit plane from the curved duct. Velocity magnitudes for each particle were calculated as the vector sum of velocity components in the horizontal plane, that is, in x and z coordinates (fig. 2). FLUENT-predicted velocity magnitudes were the basis for comparing the FLUENT simulation model results with laboratory results.

MATERIALS AND METHODS

LABORATORY SETUP

The laboratory setup consisted of a (1) curved duct made from stainless steel in the same shape as was modeled in FLUENT (fig. 2), (2) a centrifugal blower (model 4C131A, Dayton Electric Co., Chicago, Ill.) belt-driven from a 2.2 kW, 3500 rpm, 3-phase, 230 V electric motor, and (3) a small fertilizer hopper with sliding gate—used as a material feeding mechanism. The blower selected was large enough to give well over 62 m/s air speed in the curved duct. Lower air speeds were obtained by using appropriately sized pulleys. This blower had an outlet of 180 × 146 mm that was connected to the 120 × 90 mm inlet of the experimental duct through a 1-m-long convergent duct and a 30-cm-long straight duct. The purpose of having a relatively long convergent piece in the middle was to minimize turbulence in the airflow before it entered the experimental duct. The straight duct was used for measuring the air velocity and for introduction of fertilizer particles into the experimental duct. In the straight duct at its inlet end, a bundle of eighteen 19 mm diameter, 152 mm long thin wall plastic pipes was installed for further straightening the airflow.

To measure the air velocity, a pitot tube was installed in the center of the straight duct. The difference between the dynamic and the static air pressures was recorded using a differential pressure transducer (model PX170-14DV, Omega Engineering) and a data logger (model 21X, Campbell Scientific Inc.). Data obtained with the pressure transducer was double checked with a 300 mm manometer filled with water and having graduations at 3.17 mm. Air speed data were logged at one second intervals during the tests and averaged every 60 s. The air velocity measurements at the inlet of the experimental duct are summarized in table 2. In FLUENT simulations of the curved duct, the same four air velocities were used as the u-velocity at the inlet.

PARTICLE VELOCITY MEASUREMENT PROCEDURE

Urea particles retained on the sieves were saved in separate bags for use in the laboratory tests. There were not enough particles in the largest size groups of 3.66 mm from screening of urea fertilizer to complete all laboratory tests; therefore, this size group was not considered in the laboratory tests. To measure the velocity of urea particles emanating from the curved duct, a Sony charge coupled device (CCD) camera (model XC-711) was used. The images were taken at a shutter speed of 1/250 s with the camera looking down at the particles leaving the curved duct. The camera was aligned to see the upper edge of the curved duct as a horizontal line near the top in the frame. This procedure provided a frame of reference for measuring particle velocities in x and z

directions at the exit from the curved duct. The velocity component in the y direction was not measured. The images from the CCD camera were recorded for later analysis on a 8 mm tape using a Pentax video camera (model PV-C880A). Before running the tests with fertilizer particles, the picture frame was calibrated with images of a ruler placed in the curved duct. Thereafter, the camera was kept undisturbed until all tests were completed. The general procedure followed in the laboratory tests was to set the blower speed to a particular air velocity and then slowly pour urea particles from one of the bags into the fertilizer distributor mounted over the straight section near the inlet of the curved duct. Images of particles flying out of the curved duct were registered on the video tape for about five minutes. Subsequently, the fertilizer hopper was vacuumed before introducing another size particles. This process was repeated for all five particle sizes and four air speeds. Images on the video tape were identified by inserting appropriate labels for each set of observations. Particles were lit with strong light from a mini-projector (model 100-09, Berkey Colortron Inc., Burbank, Calif.) against a flat black background. The objective was to secure sharp contrast between particle traces seen in the images and the background.

DIGITIZATION AND ANALYSIS OF VIDEO IMAGES

Images from the video tape were digitized with Snappy Video Snapshot and Snappy software version 1.0 (Play Inc., Rancho Cordova, Calif.) and then analyzed with the help of Paint Shop Pro (JASC Inc., Eden Prairie, Minn.). Snappy Snapshot permits picking a picture frame from the video tape and saving it as bitmap image file. Sufficient images were saved to get velocity data on at least 15 particles for each treatment. One digitized image of the ruler provided the required calibration for the number of pixels per unit length on the real scale. The Paint Shop Pro program was used for measuring the length of particle traces in the images, in terms of pixel counts. Pixel counts were then converted into trace lengths on a real scale via the calibration factor. Once the length of a particle trace was known, the velocity was computed given the shutter speed as 1/250 s.

RESULTS AND DISCUSSION

PARTICLE VELOCITY

FLUENT-predicted particle velocities and those measured in the laboratory were analyzed as one data set to make statistical comparisons between the FLUENT simulations and laboratory results. Treatment effects from the analysis of variance are summarized in table 3. The differences among particle velocities predicted with FLUENT and those measured in the laboratory were found

Table 2. Air velocity measurements at the inlet of the curved duct

Air Velocity Level	Measured Air Velocity (m/s)	Std. Dev.	Corresponding Aircraft Airspeed* (km/s)
1	62	0.48	223
2	56	0.31	202
3	46	0.22	165
4	42	0.17	150

* Assuming the aircraft airspeed to be the same as air velocity at the inlet of the spreader.

Table 3. A summary of treatment effects on the particle exit velocity

Source	DF	Sum of Squares	F Ratio	Prob > F
Principal treatments (FLUENT versus Laboratory results)	1	635.02	721.67	< 0.0001
Air velocity	3	7161.93	2713.07	< 0.0001
Particle diameter	4	2235.62	635.17	< 0.0001
Air velocity*Particle diameter	12	38.95	3.69	< 0.0001
Air velocity*Principal treatments	3	6.42	2.43	0.064
Particle diameter*Principal treatments	4	0.56	0.16	0.9584

to be highly significant ($P \leq 0.0001$). Similarly, the air velocity at the inlet of the curved duct had a significant effect on the velocity of particles emanating from the curved duct ($P \leq 0.0001$). Particle velocities were also significantly dependent upon their geometric mean diameters. Among the interactions, the air velocity and particle diameter interaction was found to be statistically significant which meant that the particles of different sizes accelerated differently as the air velocity was changed. However, the sum of squares for the air velocity and the particle diameter interaction was very small compared to those for any of the three main effects (table 3). This suggested that even though this interaction was statistically significant, its actual effect on the particle velocity was very small relative to the individual effects of the main factors. Two other possible interactions involving these two variables with the principal treatments, were not significant. This was obvious from the fact that the particle diameter effect and the air velocity effect on the velocity of particles emanating from the duct were the same for FLUENT simulations as under the laboratory conditions.

The effect of the air velocity on the particle velocity was further analyzed using data from the laboratory tests (fig. 3). Linear regression coefficients for each of the five particle sizes are listed in table 4. The particle velocity at the exit from the duct was linearly related to the air velocity at the inlet in the range of 42 to 62 m/s. Further, at a given air velocity, the smaller particles attained higher velocities than the larger particles. These results show that if a granular material consisting of a mixture of small and

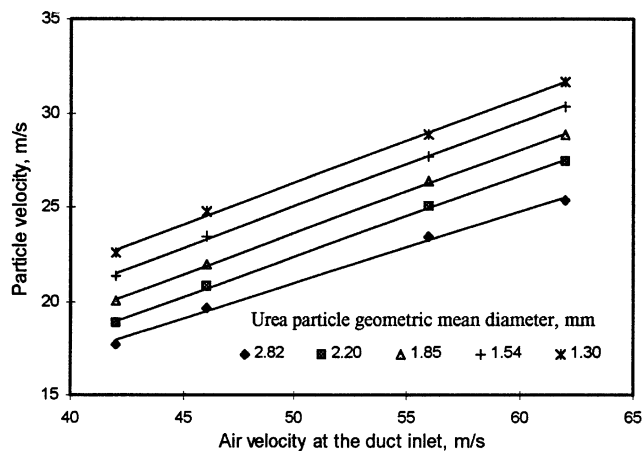


Figure 3—Mean velocity of particles in different size groups as a function of air velocity at the inlet of the curved duct.

Table 4. Linear regression coefficients for the air velocity effect on the velocity of urea particle in different sizes

Particle GMD (mm)		Intercept	Slope	R ²
2.82	Coefficient	1.99	0.38	0.99
	Std err	0.83	0.02	
2.20	Coefficient	0.94	0.43	0.99
	Std err	0.54	0.01	
1.85	Coefficient	1.53	0.44	0.99
	Std err	0.43	0.01	
1.54	Coefficient	2.74	0.45	0.99
	Std err	0.53	0.01	
1.30	Coefficient	4.14	0.44	0.99
	Std err	0.77	0.01	

large particles, as is the case usually, is fed into the aerial spreader, smaller particles would overtake larger particles causing collisions among the particles and disorder in the material flow.

Urea particle velocities predicted by FLUENT simulations were compared with the laboratory results for each air velocity (figs. 4-7). Second-order polynomial regressions gave the best fit curves for both the simulation and the laboratory results. For both FLUENT simulation data and the laboratory results, quadratic terms in the regression equations were found to be statistically significant ($P < 0.01$).

It can be seen from figures 4 to 7 that FLUENT simulations for urea in the stream of air always predicted lower particle velocities than those observed in the laboratory, irrespective of particle size and the air velocity. It is most likely because the simulation model assumes spherical shape for the particles. The actual fertilizer particles were not spherical in shape. Hence the drag coefficient for a urea particle would be higher than for a spherical particle having the same density and mass. As a result, urea particles moving with air would have more driving force acting on them than was predicted by the model.

Figures 4 to 7 also indicate that, for a given air speed, the regression curves for the laboratory results and the simulation results run almost parallel, and the vertical distance between them is nearly the same for all the air velocities. This suggests that FLUENT simulation results

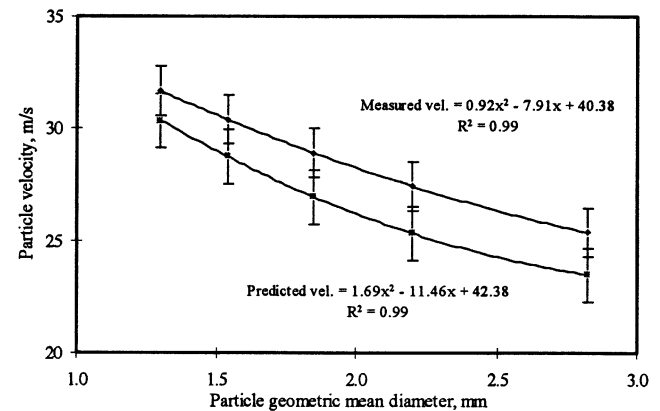


Figure 4—Comparison between predicted and measured particle velocities at 62 m/s air velocity.

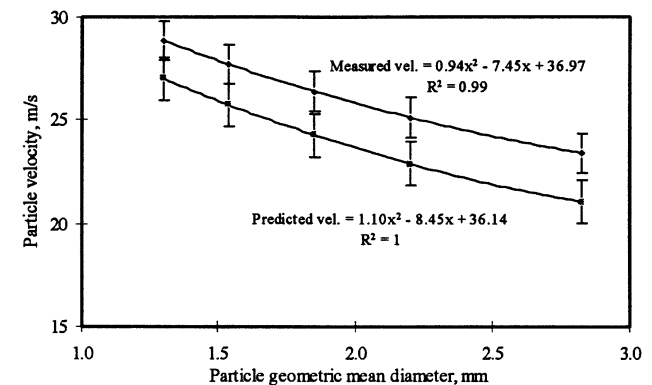


Figure 5—Comparison between predicted and measured mean particle velocities at 56 m/s air velocity.

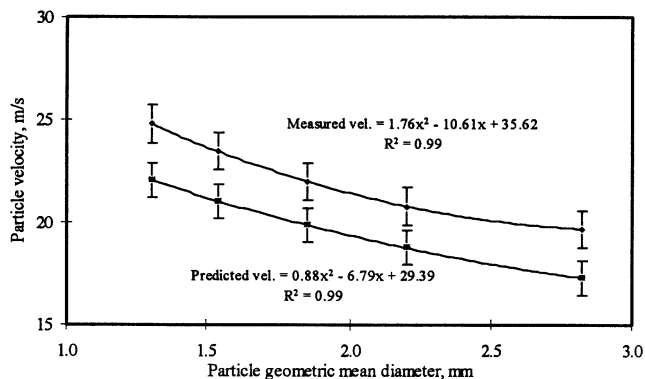


Figure 6—Comparison between predicted and measured mean particle velocities at 46 m/s air velocity.

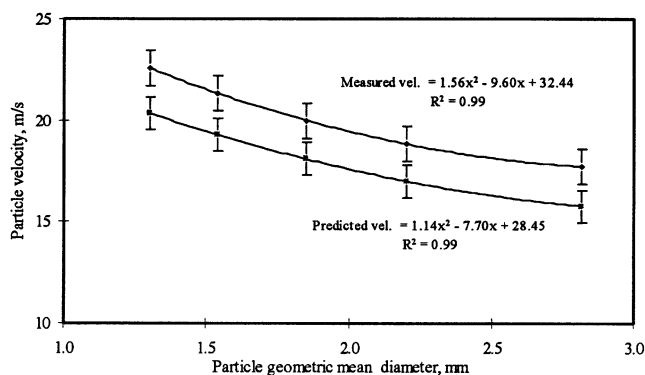


Figure 7—Comparison between predicted and measured mean particle velocities at 42 m/s air velocity.

can be corrected with a common correction factor to account for the shape of particles. One value for the correction factor could be sufficient for all particle sizes and air velocities, so long as the shape of particles does not change. This correction factor, studied in considerable detail by other researchers (West, 1972; Grift et al., 1997; Walker et al., 1997), is an aerodynamic property of particles of certain shape. Walker et al. (1997) studied the drag coefficient of urea particles along with the particles of other types of fertilizers in relation to their shape factor. The shape factor was defined as a dimensionless parameter representing the degree to which shape of a particle deviated from spherical. The drag coefficient of fertilizer particles was found to increase linearly with increasing values for the shape factor. The value of the shape factor, however, did not depend upon the particle size, meaning that smaller particles could also have a higher drag coefficient.

Particle velocity correction factors calculated as the ratio of mean measured velocity and the mean FLUENT-predicted velocity for different particle sizes and air velocities are plotted in figure 8. The correction factor varied from 1.04 to 1.14 with a mean of 1.09 (Standard deviation = 0.025). It did not seem to depend upon the particle size in 1.3 to 2.82 mm range, because the effect of particle size on the correction factor did not show any trend in figure 8. However, the correction factor was less for higher air velocities perhaps because the particles remained in contact with high velocity air for smaller duration.

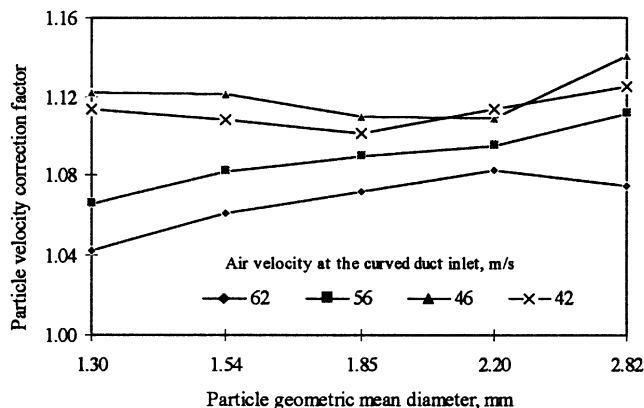


Figure 8—Mean particle velocity correction factors calculated for different particle sizes and air velocities.

Because the laboratory tests were conducted with air velocities in the range of those expected during the aerial application of urea, the average correction factor of 1.09 could be used on FLUENT simulation results for an aerial spreader to calculate the velocity of particles.

PARTICLE FLOW PATTERN

Dispersed phase simulation in FLUENT calculates the trajectory of individual particles injected at any location in the flow stream inside the computational domain. Based on the trajectory calculations, FLUENT plots particle concentration contours at selected cross sections perpendicular to the main flow direction. Figure 9 shows the concentration of urea particles at selected planes across the curved duct. In the simulations, a total of 75 particles were injected in the air stream at the front end just below the top edge of the duct. Simulation results show that at the first few planes following the inlet plane, the concentration of particles roughly follows the pattern in which they were introduced in the duct. However, quite soon thereafter the particles from the upper layers move down due to the gravitational force and bounce against the bottom or the outer side wall. FLUENT results suggest that all particles move along the lower portion of the outer wall and exit from the lower right corner. The laboratory results appeared to support the FLUENT predictions for particle trajectories inside the curved duct. Images taken by the camera looking down at the particles emanating from the curved duct showed far more particles coming out along the outer wall and very few particles emanating from the middle portion or near the inner side wall of the curved duct. Some particles did not follow the main stream flow due to their bouncing against the duct walls or collision with other particles.

CONCLUSIONS

The flow of air and urea particles in a curved duct resembling the left duct of an aerial spreader was successfully modeled with the FLUENT dispersed phase model. FLUENT-predicted particle velocities at the exit end of the curved duct were compared with laboratory measurements. FLUENT consistently predicted lower particle velocities than observed in the laboratory. The difference was attributed to the non-spherical shape of the

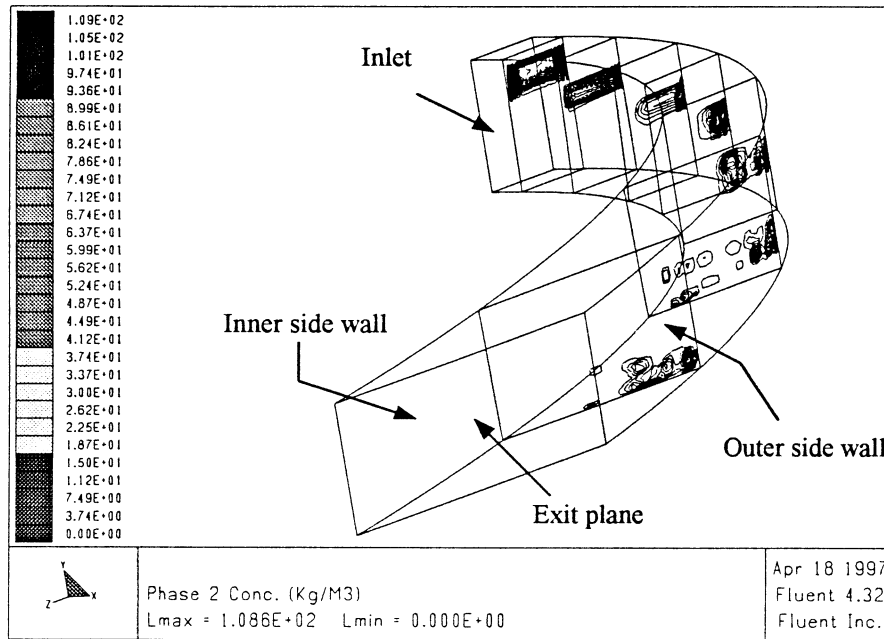


Figure 9—Urea particle concentration contours at selected vertical planes across the length of the curved duct.

particles which would result in higher drag coefficients for the particles, and actual velocities higher than predicted velocities. The effect of the particle shape necessitates a correction factor on the particle velocities predicted by the model. In the case of urea, predicted velocities need to be raised by 9% to obtain realistic velocities. This correction factor was found to be independent of particle size and the air velocity. However, for other materials having particles of different shape, a different correction factor will be required.

ACKNOWLEDGMENTS. The authors thank Dr. Yang Tao, Assistant Professor, Biological and Agricultural Engineering Department, Dr. Michael B. Stewart, Assistant Professor, and Dr. Arnoldo Muyschondt, Assistant Professor, Mechanical Engineering Department, University of Arkansas, Fayetteville for their technical assistance.

REFERENCES

Akesson, N. B., and W. E. Yates. 1964. Airplane application of bulk fertilizer. *Transactions of the ASAE* 7(2):137-141.

ASAE Standards, 38th Ed. 1991. S319.1. Method of determining and expressing fineness of feed materials by sieving. St. Joseph, Mich.: ASAE.

Bilanin, A. J., M. E. Teske, J. W. Berry, and R. E. Ekbald. 1989. AGDISP: The aircraft spray dispersion model, code development and experimental validation. *Transactions of the ASAE* 32(1):327-334.

Bilanski, W. K., S. H. Collins, and P. Chu. 1962. Aerodynamic properties of seed grains. *Agricultural Engineering* 43(4):216-219.

Brazelton, R. W., N. B. Akesson, and W. E. Yates. 1968. Dry materials distribution by aircraft. *Transactions of the ASAE* 11(5):635-641.

Durst, F., D. Milojevic, and B. Schonung. 1984. Eulerian and Lagrangian predictions of particulate two-phase flows: A numerical study. *Applied Math. Model.* 8(2):101-115.

Fluent Incorporated. 1995. *FLUENT User's Guide*, Vol. 1-4. Lebanon, N.H.: Fluent Inc.

Gardisser, D. R., and J. T. Walker. 1990. Adjustment of granular spreaders on agricultural aircraft. ASAE Paper No. AA90-003. St. Joseph, Mich.: ASAE.

Griffis, C. L., D. W. Ritter, and E. J. Matthews. 1983. Simulation of rotary spreader distribution pattern. *Transactions of the ASAE* 26(1):33-37.

Grift, T. E., J. T. Walker, and J. W. Hofstee. 1997. Aerodynamic properties of individual fertilizer particles. *Transactions of the ASAE* 40(1):13-20.

Henry, J. E. 1962. Study of distributors for applying dry material by airplane. Ohio Agricultural Experimental Station Research Bulletin 906. May. Wooster, Ohio: Ohio Agric. Experiment Station.

Hoffmeister, G. 1979. Physical properties of fertilizers and methods of measuring them. Bulletin Y-147. Muscle Shoals, Ala.: Nat. Fertilizer Development Center, Tennessee Valley Authority.

Hofstee, J. W. 1992. Handling and spreading of fertilizers. Part 2: Physical properties of fertilizer, measuring methods and data. *J. Agric. Engng. Res.* 53(2):141-162.

Law, S. E., and J. A. Collier. 1973. Aerodynamic resistance coefficients of agricultural particles determined by elutriation. *Transactions of the ASAE* 16(5):918-921.

Mennel, R. M., and A. R. Reece. 1963. The theory of centrifugal distributors. III: Particle trajectories. *J. Agric. Engng. Res.* 8(1): 78-854.

Texas A&M University. 1956. *Handbook of Aerial Application in Agriculture: A Compilation of Information Emanating from Research and Conferences*. Available from Texas Agricultural Extension Service, College Station, Texas.

Walker, J. T., and D. R. Gardisser. 1989. Using AGDISP for dry material deposition analysis. ASAE Paper No. AA89-006. St. Joseph, Mich.: ASAE.

Walker, J. T., T. E. Grift, and J. W. Hofstee. 1997. Determining effects of fertilizer particle shape on aerodynamic properties. *Transactions of the ASAE* 40(1):21-27.

West, N. L. 1972. Aerodynamics force predictions. *Transactions of the ASAE* 1972(2):584-587.